














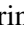


LETTER TO THE EDITOR

## HD 110067 c has an aligned orbit

### Measuring the Rossiter–McLaughlin effect inside a resonant multi-planet system with ESPRESSO

J. Zak<sup>1,2,3</sup> , H. M. J. Boffin<sup>1</sup> , E. Sedaghati<sup>4</sup> , A. Bocchieri<sup>5</sup> , Q. Changeat<sup>6</sup>, A. Fukui<sup>7,8</sup>, A. Hatzes<sup>9</sup> , T. Hillwig<sup>10</sup>, K. Hornoch<sup>2</sup> , D. Itrich<sup>11</sup> , V. D. Ivanov<sup>1</sup> , D. Jones<sup>8,12,13</sup> , P. Kabath<sup>2</sup> , Y. Kawai<sup>14</sup>, L. V. Mugnai<sup>15</sup> , F. Murgas<sup>8,12</sup>, N. Narita<sup>7,16</sup> , E. Palle<sup>8,12</sup>, E. Pascale<sup>5</sup>, P. Pravec<sup>2</sup>, S. Redfield<sup>17</sup> , G. Roccetti<sup>1,18</sup>, M. Roth<sup>3,9</sup> , J. Srba<sup>2</sup>, Q. Tian<sup>17</sup> , A. Tsiaras<sup>19</sup>, D. Turrini<sup>20</sup> , and J. P. Vignes<sup>21</sup>

<sup>1</sup> European Southern Observatory, Karl-Schwarzschild-str. 2, 85748 Garching, Germany  
e-mail: [jiri.zak@eso.org](mailto:jiri.zak@eso.org)

<sup>2</sup> Astronomical Institute of the Czech Academy of Sciences, Fričova 298, 25165 Ondřejov, Czech Republic

<sup>3</sup> Faculty of Physics and Astronomy, Friedrich-Schiller-Universität, Fürstengraben 1, 07743 Jena, Germany

<sup>4</sup> European Southern Observatory, Casilla 13, Vitacura, Santiago, Chile

<sup>5</sup> Dipartimento di Fisica, La Sapienza Università di Roma, Piazzale Aldo Moro 5, Roma 00185, Italy

<sup>6</sup> European Space Agency (ESA), ESA Office, Space Telescope Science Institute (STScI), Baltimore, MD 21218, USA

<sup>7</sup> Komaba Institute for Science, The University of Tokyo, 3-8-1 Komaba, Meguro, Tokyo 153-8902, Japan

<sup>8</sup> Instituto de Astrofísica de Canarias, 38205 La Laguna, Tenerife, Spain

<sup>9</sup> Thueringer Landessternwarte Tautenburg, Sternwarte 5, 07778 Tautenburg, Germany

<sup>10</sup> Department of Physics and Astronomy, Valparaiso University, Valparaiso, IN 46383, USA

<sup>11</sup> Steward Observatory, The University of Arizona, Tucson, AZ 85721, USA

<sup>12</sup> Departamento de Astrofísica, Universidad de La Laguna, 38206 La Laguna, Tenerife, Spain

<sup>13</sup> Nordic Optical Telescope, Rambla José Ana Fernández Pérez 7, 38711 Breña Baja, Spain

<sup>14</sup> Department of Multi-Disciplinary Sciences, Graduate School of Arts and Sciences, The University of Tokyo, 3-8-1 Komaba, Meguro, Tokyo 153-8902, Japan

<sup>15</sup> School of Physics and Astronomy, Cardiff University, Queens Buildings, The Parade, Cardiff CF24 3AA, UK

<sup>16</sup> Astrobiology Center, 2-21-1 Osawa, Mitaka, Tokyo 181-8588, Japan

<sup>17</sup> Astronomy Department and Van Vleck Observatory, Wesleyan University, Middletown, CT 06459, USA

<sup>18</sup> Department of Physics, Ludwig-Maximilian University of Munich, Geschwister-Scholl-Platz 1, 80539 Munich, Germany

<sup>19</sup> Department of Physics and Astronomy, University College London, Gower Street, WC1E 6BT London, UK

<sup>20</sup> INAF – Osservatorio Astrofisico di Torino, Via Osservatorio 20, 10025 Pino Torinese, Italy

<sup>21</sup> American Association of Variable Star Observers, Cambridge, USA

Received 30 April 2024 / Accepted 24 May 2024

#### ABSTRACT

Planetary systems in mean motion resonances hold a special place among the planetary population. They allow us to study planet formation in great detail as dissipative processes are thought to have played an important role in their existence. Additionally, planetary masses in bright resonant systems can be independently measured via both radial velocities and transit timing variations. In principle, they also allow us to quickly determine the inclination of all planets in the system since, for the system to be stable, they are likely all in coplanar orbits. To describe the full dynamical state of the system, we also need the stellar obliquity, which provides the orbital alignment of a planet with respect to the spin of its host star and can be measured thanks to the Rossiter–McLaughlin effect. It was recently discovered that HD 110067 harbors a system of six sub-Neptunes in resonant chain orbits. We here analyze an ESPRESSO high-resolution spectroscopic time series of HD 110067 during the transit of planet c. We find the orbit of HD 110067 c to be well aligned, with a sky-projected obliquity of  $\lambda = 6^{+24}_{-26}$  deg. This result indicates that the current architecture of the system was reached through convergent migration without any major disruptive events. Finally, we report transit-timing variation in this system as we find a significant offset of  $19 \pm 4$  min in the center of the transit compared to the published ephemeris.

**Key words.** techniques: radial velocities – planets and satellites: gaseous planets – planet-star interactions – planets and satellites: individual: HD 110067

#### 1. Introduction

Resonant planetary chains consist of three or more planets in the same system with integer period ratios. Their config-

uration is highly indicative of dissipative processes having played an important role during their formation (Lissauer et al. 2011; Kley & Nelson 2012; Pichierri et al. 2019). One of the main proposed channels of planet formation is core accretion

coupled with disk migration (Goldreich & Tremaine 1980; Terquem & Papaloizou 2007; Coleman & Nelson 2016). During their formation, planetary embryos migrate inward due to torques from the gaseous disk. Migration is halted by the planet disk–edge interaction, and other embryos migrate into a resonant chain. Current simulations predict that as gas disks dissipate, only around 50–60% of resonant chains become unstable (Izidoro et al. 2017). This is in clear contrast to the observed population, where only a few percent of *Kepler* multi-planet systems are near first-order resonance (Fabrycky et al. 2014). Hence, further investigations of these few systems in resonance are highly warranted to explain why only such a small number of systems that retained their peculiar resonant architecture have so far been detected. Several mechanisms that might be responsible for breaking the resonances at an early stage have been proposed, such as over-stable librations (Deck & Batygin 2015), nontidal secular processes (Hamer & Schlaufman 2024), or changes in the migration rate (Kanagawa & Szuszkiewicz 2020). Thus, the question arises as to how these few resonant systems managed to keep their peculiar architecture. Recently, by analyzing 11 resonant chain systems, Wong & Lee (2024) found an empirical relation that supports the idea that the resonant chains are formed and maintained by the stalling of the migration of the innermost planet near the inner edge of the disk, which is truncated by the magnetic fields of the protostar. However, further investigation is needed to assess the universality of this mechanism.

Planetary systems can end up with similar observable properties despite different formation and migration histories (Dawson & Johnson 2018). By measuring the spin–orbit alignment, in addition to the eccentricity and stellar inclination, we can infer fundamental aspects of their evolutionary history (Campante et al. 2016; Muñoz & Perets 2018; Rice et al. 2022). In particular, the sky-projected orbital obliquity, which represents the angle between a planet’s orbital angular momentum and its host star’s spin axis, gives invaluable clues on the dynamical evolution of multi-planet systems and their interactions with the protoplanetary disk or other bodies (Matsakos & Königl 2017).

To measure this quantity, one can utilize the Rossiter–McLaughlin (R–M) effect (Rossiter 1924; McLaughlin 1924). Since the first detection of the R–M effect of a hot Jupiter (Queloz et al. 2000), over 250 systems have had their stellar obliquity characterized (e.g., Albrecht et al. 2022; Zak et al. 2024). The observed population of exoplanets has a diverse distribution of orbits (Siegel et al. 2023). Early studies had initially shown most multi-planet systems having aligned orbits (Albrecht et al. 2013), but, since then, several multi-planet systems with significant misalignment have been found (e.g. Dalal & Hébrard 2019; Hjorth et al. 2021). Several mechanisms have been proposed to explain misalignment in multi-planet systems, for example primordial misalignment and gravitational perturbations from stellar- or planetary-mass companions. Esteves et al. (2023) show that secular perturbations of cold gas giants alone cannot account for the obliquity distribution of low-mass exoplanets.

When planetary systems have architectures in resonant equilibrium, this indicates they have not been subject to any major dynamical rearrangements since their formation (Fang & Margot 2012). Therefore, they provide an unparalleled opportunity to probe the primordial obliquities of planet-hosting stars, as coplanarity does not automatically produce alignment between the planetary orbital plane and the stellar spin axis. Rice et al. (2023) studied the distribution of the 3D spin–orbit alignment ( $\psi$ ) of resonant and near-resonant systems and conclude that the observed distribution of the obliquity is not consis-

**Table 1.** Properties of the host star and planet c in the HD 110067 system.

	Parameter	Value
Star	$V$ magnitude	8.4
	Sp. type	K0
	$M_s$ ( $M_\odot$ )	$0.80 \pm 0.04$
	$R_s$ ( $R_\odot$ )	$0.788 \pm 0.008$
	$T_{\text{eff}}$ (K)	$5266 \pm 64$
	$v \sin i_*$ ( $\text{km s}^{-1}$ )	$2.5 \pm 1.0$
Planet c	$M_p$ ( $M_\oplus$ )	$<6.3$
	$K_p$ ( $\text{m s}^{-1}$ )	$<1.55$
	$R_p$ ( $R_\oplus$ )	$2.388 \pm 0.036$
	$R_p/R_s$	$0.0278 \pm 0.0003$
	Period (d)	$13.673694 \pm 2.4 \times 10^{-5}$
	$T_0 - 2\,457\,000$ (d)	$2657.4570 \pm 0.0007$
	$a$ (au)	$0.1039 \pm 0.0013$
	$i$ (deg)	$89.687 \pm 0.163$
	$T_{\text{eq}}$ (K)	$699 \pm 9$

**Notes.** Values taken from Luque et al. (2023).

tent with near-exact alignment ( $\psi < 5$  deg). Due to their scarcity, faint host stars, and/or low amplitude of the R–M effect, only two systems in a resonant chain with more than four planets have had their obliquity determined so far. Finally, these systems offer us a comparison to our own Solar System, which has an aligned plane to within seven degrees of the solar spin axis. Such a comparison will help us understand the arrangement and distribution of various planetary systems as well as to understand the origin of the Solar System architecture and assess its uniqueness (Mishra et al. 2023).

## 2. HD 110067

HD 110067 hosts six sub-Neptune planets in resonant chain orbits (Luque et al. 2023). The orbital periods span from 9 to 55 days. HD 110067 c is the second closest planet and is on a 13-day orbit with an equilibrium temperature of 700 K. The host star and planetary properties are reported in Table 1.

As HD 110067 is the brightest known multi-planet system with more than four planets, it is a prime target for future transmission spectroscopy observations with JWST. They will determine the atmospheric molecular abundance ratios, which are indicators of the formation and evolution of planetary systems (Turrini et al. 2021). Such a comprehensive characterization is generally limited to gas giant exoplanets (Changeat et al. 2022) and will remain elusive for the TRAPPIST-1 system since the planets do not have thick atmospheres (Zieba et al. 2023). Hence, HD 110067 is the best target for studying resonant chain systems using both obliquity and atmospheric characterization in great detail.

## 3. ESPRESSO spectroscopy observations

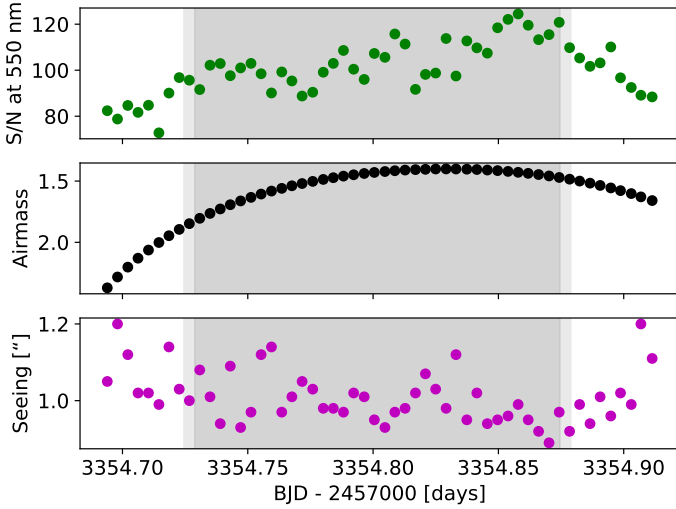
HD 110067 was observed during the transit of planet c on 14 February 2024 with the Echelle Spectrograph for Rocky Exoplanets and Stable Spectroscopic Observations (ESPRESSO)<sup>1</sup> (Pepe et al. 2021) at the incoherent combined Coude focus of ESO’s Very Large Telescope on Cerro Paranal, Chile. We used

<sup>1</sup> ESO program 112.26X6 (PI: Zak).

**Table 2.** Observing log for the ESPRESSO dataset of HD 110067.

Date	No. obs	Exp. time (s)	Airmass range	$S/N$ at 550 nm
2024-02-14	53 (37)	300	2.41–1.40–1.67	72.8–124.4

**Notes.** The number in parentheses represents the number of frames taken in transit.



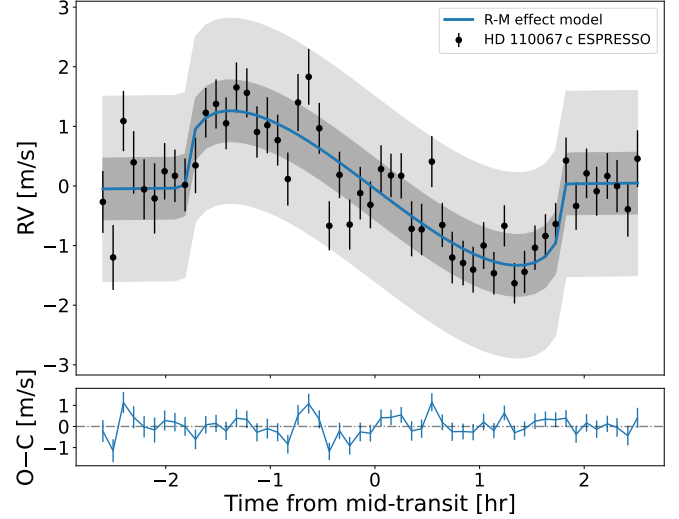
**Fig. 1.** Transit observation information. Top: signal-to-noise ratio of the ESPRESSO data at 550 nm, measured by the pipeline. (Middle) Airmass of the target during the observations. Bottom: seeing during the observations delivered at the detector and corrected for the airmass. Light gray areas indicate the partial transit duration, while dark gray shows the duration of the full transit.

the high-resolution 1-UT mode ( $\mathcal{R} \sim 140\,000$ ), reading out the detector in the  $2 \times 1$  binning setup. The readout time was 68 s. The main science fiber, A, was placed on the target, while fiber B was used to obtain simultaneous spectra of the sky background. The instrument covers the wavelength range from 380 to 788 nm. During the night, 53 spectra were obtained, each with an exposure time of 300 s. None of the other planets in the HD 110067 system were transiting during the observations. The observation log is displayed in Table 2 and Fig. 1. The data were reduced using version 3.1.0 of the ESPRESSO pipeline<sup>2</sup>. The radial velocity (RV) measurements together with their uncertainties were obtained using the ESPRESSO Data Reduction Software (DRS) pipeline, through the fitting of a Gaussian function to the cross-correlation function (CCF) with the K0 spectral mask. Alongside the spectroscopy, simultaneous photometry was obtained, but we were not able to detect any signal from the transiting planet; the description of the photometry is presented in Appendix A.

#### 4. Analysis

The obtained stellar RVs clearly show the anomaly produced by the R–M effect (Fig. 2). To measure the projected stellar obliquity of the system ( $\lambda$ ), we fit the RVs with a composite model, which includes a Keplerian orbital component as well as the R–M anomaly. This model is implemented in the

<sup>2</sup> <https://ftp.eso.org/pub/dfs/pipelines/instruments/espRESSO/espdr-pipeline-manual-3.1.0.pdf>



**Fig. 2.** R–M effect of HD 110067 c observed with ESPRESSO. The measured data points (black) are shown with their error bars. The blue line shows the model that fits the data best, together with the  $1\sigma$  (dark gray) and  $3\sigma$  (light gray) confidence intervals. The systemic velocity was removed for better visibility.

AROME<sup>3</sup> (Sedaghati et al. 2023) package, which utilizes the RADVEL python module (Fulton et al. 2018) for the formulation of the Keplerian orbit. AROME<sup>3</sup> is a Python implementation of the R–M anomaly described in the AROME code (Boué et al. 2013). We used the R–M effect function defined for RVs determined through the cross-correlation technique in our code. We set wide uniform priors for the RV semi-amplitude ( $K$ ) and the systemic velocity ( $\gamma$ ). In the R–M effect model, we fixed the following parameters to values reported in the literature: the orbital period ( $P$ ) and the eccentricity to a circular orbit ( $e$ ). The parameter  $\sigma$ , which is the width of the CCF and represents the effects of the instrumental and turbulent broadening, was measured on the data and fixed to  $\sigma = 6.60 \text{ km s}^{-1}$ . Furthermore, we used the ExoCTK<sup>4</sup> tool to compute the quadratic limb-darkening coefficients with ATLAS9 model atmospheres (Castelli & Kurucz 2003) in the wavelength range of the ESPRESSO instrument (380–788 nm). We used the limb-darkening coefficients  $u_1 = 0.564$  and  $u_2 = 0.145$ . We set Gaussian priors from the discovery paper (Luque et al. 2023) on the following parameters during the fitting procedure: the central transit time ( $T_c$ ), the orbital inclination ( $i$ ), the scaled semi-major axis ( $a/R_s$ ), and the planet-to-star radius ratio ( $R_p/R_s$ ). Uniform priors were set on the projected stellar rotational velocity ( $v \sin i_*$ ) and the sky-projected angle between the stellar rotation axis and the normal of the orbital plane ( $\lambda$ ). To obtain the best fitting values of the parameters, we employed three independent Markov chain Monte Carlo (MCMC) simulations, each with 250 000 steps, burning the first

<sup>3</sup> <https://github.com/esedagha/AROMEpy>

<sup>4</sup> <https://github.com/ExoCTK/exoctx>

**Table 3.** MCMC analysis results.

Parameter	Prior	Result
$T_c - 2\,460\,000$ (d)	$\mathcal{N}(T_0 \pm 0.01)$	$354.8018^{+0.0020}_{-0.0022}$
$\lambda$ (deg)	$\mathcal{U}(-180, 180)$	$6^{+24}_{-26}$
$v \sin i_*$ (km s <sup>-1</sup> )	$\mathcal{U}(0, 5)$	$1.39^{+0.26}_{-0.19}$
$R_p/R_s$	$\mathcal{N}(0.0278, 0.0003)$	$0.0278 \pm 0.0003$
$a/R_s$	$\mathcal{N}(28.37, 0.30)$	$28.52^{+0.29}_{-0.30}$
$i$ (deg)	$\mathcal{N}(89.687, 0.163)$	$89.64^{+0.19}_{-0.17}$
$\gamma$ (km s <sup>-1</sup> )	$\mathcal{U}(-8.48, -8.58)$	$-8.5306 \pm 0.0001$
$K$ (km s <sup>-1</sup> )	$\mathcal{U}(-0.02, 0.02)$	$-0.001 \pm 0.003$

**Notes.**  $\mathcal{N}$  denotes priors with a normal distribution and  $\mathcal{U}$  priors with a uniform distribution.

50 000. The results of the MCMC simulations are presented in Table 3 and in Figs. 2 and B.1.

## 5. An aligned system with small TTVs

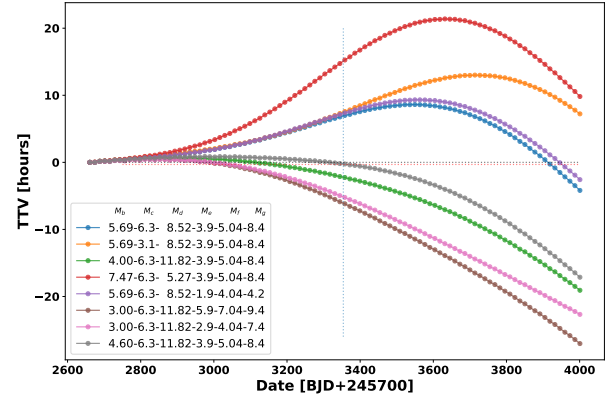
From our analysis, we find a well-aligned orbit for HD 110067 c with a sky-projected obliquity of  $\lambda = 6^{+24}_{-26}$  degrees. Such a high state of alignment indicates that the architecture of the system was reached through convergent migration without any major disruptive events (if we make the reasonable assumption that all the planets share the same value of  $\lambda$ ). We ran a numerical simulation with one planet inclined, and such a system does not lead to a set of six transiting exoplanets. Given the tidal circularization timescale of planet c ( $\tau_{\text{circ}} \gg 14$  Gyr; Goldreich & Soter 1966), we can also rule out that the orbit of planet c was temporarily excited by an event and later realigned, thereby confirming the quiescent evolution of the system.

We detect a scatter (just before the middle of the transit) in the observed RV data that we were not able to fully describe in our model, although it is not very significant (within the  $3\sigma$  interval of our model). To investigate the origin of this scatter, we checked the spectral CCF indices (Hatzes 2019) provided by the ESPRESSO DRS pipeline (e.g., the full width at half maximum and the bisector span) as well as the  $\log R'_{\text{HK}}$  activity index provided by the Data Analysis Software (DAS) pipeline<sup>5</sup>, which is indicative of stellar activity originating in the chromosphere. Finally, the  $H\alpha$  index was measured using the Activity Indices Toolkit (ACTIN2) code<sup>6</sup>. We do not find any correlation in any of the indices with the RV residuals. We show the derived values of  $\log R'_{\text{HK}}$  in Fig. B.2 together with the RV residuals. The data show no significant deviations from the mean value throughout the night, suggesting that chromospheric activity is not responsible for the scatter. The scatter could be caused by the planet crossing a stellar spot. However, despite having multiple photometry datasets, we were not able to detect any features indicative of spot-crossing.

Our derived center of the transit is  $19 \pm 4$  min earlier than what is expected from the calculated ephemeris, while the propagated uncertainty is only 3 min (Luque et al. 2023). Such a significant deviation hints at transit-timing variation (TTV), which is not a surprise in a system with six planets. TTVs are observed

<sup>5</sup> <https://www.eso.org/sci/software/pipelines/espresso-das/espresso-das-pipe-recipes.html>

<sup>6</sup> <https://github.com/gomesdasilva/ACTIN2>



**Fig. 3.** Estimated TTVs for planet c in the system, for various planet masses, as indicated in the legend. The dashed vertical line marks the observing time with ESPRESSO. The dotted horizontal lines indicate no TTV (black) and a 19 min TTV (red).

in similar multi-planet systems such as TRAPPIST-1, TOI-178, and TOI-1136 (Teyssandier et al. 2022; Delrez et al. 2023; Beard et al. 2024).

Constraining the amplitude of the TTVs is rather difficult with such a weak constraint on the planetary masses (Lammers & Winn 2024). Nevertheless, we ran numerical simulations using REBOUND (Rein & Liu 2012), finding that TTVs of up to tens of hours could be expected starting from the time of the published ephemeris. In this sense, having caught the transit with such a small TTV seems lucky, even if it is consistent with the reported non-detection of TTVs in two years of Transiting Exoplanet Survey Satellite (TESS, Ricker et al. 2015) observations (Luque et al. 2023). The masses in the system are not well known, however – for some of them, only upper limits exist. This leads to a rather large range of variations in the expected TTVs for planet c, as shown in Fig. 3. Some combination of masses would explain the small amount of TTVs since the previous ephemeris. However, as the solution is clearly degenerate, more transit times are needed to confirm this. Such TTVs need to be taken into account when planning future atmospheric follow-up during, for example, JWST Cycle 4 or with Ariel to avoid wasting valuable telescope time.

In the inside-out planet formation scenario (Chatterjee & Tan 2014), the planets closest to the host star formed first, with those on farther orbits forming later. In this regard, planets farther from their host stars with weaker tidal forces offer us an even better opportunity to search for possible evidence of any perturbations. However, notable exceptions are systems such as K2-266 (Rodríguez et al. 2018), which hosts at least three coplanar planets on short orbits and one ultrashort-period planet ( $\sim 0.7$  days). The innermost planet, with its lower inclination ( $\sim 75$  deg), significantly deviates from the orbital configuration of the other planets in the system, which have inclinations above 87 deg. Such an orbital configuration suggests a different evolutionary pathway for the innermost planet (Becker et al. 2020).

Spin-orbit measurements of multi-planet resonant chain systems with more than four planets are very sparse, with only two studied systems. TRAPPIST-1 was studied by Hirano et al. (2020), who found the system to be well aligned from a joint analysis of three planets in the system. An aligned orbit was later confirmed by Brady et al. (2023), who derived an obliquity of the system of  $\lambda = 2^{+17}_{-19}$  deg. Dai et al. (2023) derived an aligned orbit,  $\lambda = 5 \pm 5$  deg, for planet d in the sextuplet system

TOI-1136. Together with the well-aligned orbit of HD 110067 c, such a preliminary trend among resonant chains might support a proposition made by Esteves et al. (2023), that primordial misalignment may have a key role in triggering dynamical instabilities after gas disk dispersal.

We encourage further investigations of the HD 110067 system. Due to the larger R–M effect amplitudes of planets d, f, and g (compared to b, c, and e), these planets are amenable to future measurement of the obliquity with even higher precision, possibly allowing us to detect Solar System-like deviation from an aligned state (Beck & Giles 2005). Such measurements will provide the (mis)alignment between two or more planets in the resonant chain system with high confidence for the first time. Furthermore, such studies will also complement photometric studies that use TTVs to obtain precise masses of this system, independently of the RV method. This will aid in understanding the observed discrepancy in the literature between planetary masses derived using the RV and TTV methods (Mills & Mazeh 2017; Adibekyan et al. 2024).

**Acknowledgements.** The authors would like to thank the anonymous referee for their insightful report. J.Z., P.K. and J.S. acknowledge the support from GACR:22-30516K. D.J. acknowledges support from the Agencia Estatal de Investigación del Ministerio de Ciencia, Innovación y Universidades (MCIU/AEI) and the European Regional Development Fund (ERDF) with reference PID-2022-136653NA-I00 (DOI:10.13039/501100011033). D.J. also acknowledges support from the Agencia Estatal de Investigación del Ministerio de Ciencia, Innovación y Universidades (MCIU/AEI) and the European Union NextGenerationEU/PRTR with reference CNS2023-143910 (DOI:10.13039/501100011033). A.B. is supported by the Italian Space Agency (ASI) with Ariel grant n. 2021.5.HH.0. We acknowledge financial support from the Agencia Estatal de Investigación del Ministerio de Ciencia e Innovación MCIN/AEI/10.13039/501100011033 and the ERDF “A way of making Europe” through project PID2021-125627OB-C32, and from the Centre of Excellence “Severo Ochoa” award to the Instituto de Astrofísica de Canarias. Work of K.H. and P.P. was supported by the project RVO:67985815. Based (in part) on data collected with the Danish 1.54-m telescope at the ESO La Silla Observatory. D.I. acknowledges support from collaborations and/or information exchange within NASA’s Nexus for Exoplanet System Science (NExSS) research coordination network sponsored by NASA’s Science Mission Directorate under Agreement No. 80NSSC21K0593 for the program “Alien Earths”. This work is partly supported by JST SPRING, Grant Number JPMJSP2108.

## References

- Adibekyan, V., Sousa, S. G., Delgado Mena, E., et al. 2024, *A&A*, **683**, A159
- Albrecht, S., Winn, J. N., Marcy, G. W., et al. 2013, *ApJ*, **771**, 11
- Albrecht, S. H., Dawson, R. I., & Winn, J. N. 2022, *PASP*, **134**, 082001
- Andersen, J., Andersen, M. I., Klougart, J., et al. 1995, *Messenger*, **79**, 12
- Beard, C., Robertson, P., Dai, F., et al. 2024, *AJ*, **167**, 70
- Beck, J. G., & Giles, P. 2005, *ApJ*, **621**, L153
- Becker, J., Batygin, K., Fabrycky, D., et al. 2020, *AJ*, **160**, 254
- Boué, G., Montalto, M., Boisse, I., et al. 2013, *A&A*, **550**, A53
- Brady, M., Bean, J. L., Seifahrt, A., et al. 2023, *AJ*, **165**, 129
- Campante, T. L., Lund, M. N., Kuszlewicz, J. S., et al. 2016, *ApJ*, **819**, 85
- Castelli, F., & Kurucz, R. L. 2003, in *Modelling of Stellar Atmospheres*, eds. N. Piskunov, W. W. Weiss, & D. F. Gray, 210, A20
- Changeat, Q., Edwards, B., Al-Refai, A. F., et al. 2022, *ApJS*, **260**, 3
- Chatterjee, S., & Tan, J. C. 2014, *ApJ*, **780**, 53
- Coleman, G. A. L., & Nelson, R. P. 2016, *MNRAS*, **457**, 2480
- Dai, F., Masuda, K., Beard, C., et al. 2023, *AJ*, **165**, 33
- Dalal, S., Hébrard, G., Lecavelier des Étangs, A., et al. 2019, *A&A*, **631**, A28
- Dawson, R. I., & Johnson, J. A. 2018, *ARA&A*, **56**, 175
- Deck, K. M., & Batygin, K. 2015, *ApJ*, **810**, 119
- Delrez, L., Leleu, A., Brandeker, A., et al. 2023, *A&A*, **678**, A200
- Esteves, L., Izidoro, A., Winter, O. C., et al. 2023, *MNRAS*, **521**, 5776
- Fabrycky, D. C., Lissauer, J. J., Ragozzine, D., et al. 2014, *ApJ*, **790**, 146
- Fang, J., & Margot, J.-L. 2012, *ApJ*, **761**, 92
- Fulton, B. J., Petigura, E. A., Blunt, S., et al. 2018, *PASP*, **130**, 044504
- Goldreich, P., & Soter, S. 1966, *Icarus*, **5**, 375
- Goldreich, P., & Tremaine, S. 1980, *ApJ*, **241**, 425
- Hamer, J. H., & Schlaufman, K. C. 2024, *AJ*, **167**, 55
- Hatzes, A. P. 2019, *The Doppler Method for the Detection of Exoplanets* (Bristol, UK: IOP Publishing)
- Hirano, T., Gaidos, E., Winn, J. N., et al. 2020, *ApJ*, **890**, L27
- Hjorth, M., Albrecht, S., Hirano, T., et al. 2021, *Proc. Natl. Acad. Sci.*, **118**, e2017418118
- Izidoro, A., Ogihara, M., Raymond, S. N., et al. 2017, *MNRAS*, **470**, 1750
- Kanagawa, K. D., & Szuszkiewicz, E. 2020, *ApJ*, **894**, 59
- Keel, W. C., Oswalt, T., Mack, P., et al. 2017, *PASP*, **129**, 015002
- Keel, W. C., Oswalt, T., Mack, P., et al. 2021, *PASP*, **133**, 069201
- Kley, W., & Nelson, R. P. 2012, *ARA&A*, **50**, 211
- Lammers, C., & Winn, J. N. 2024, *ApJ*, **968**, L12
- Lissauer, J. J., Ragozzine, D., Fabrycky, D. C., et al. 2011, *ApJS*, **197**, 8
- Lique, R., Osborn, H. P., Leleu, A., et al. 2023, *Nature*, **623**, 932
- Matsakos, T., & Königl, A. 2017, *AJ*, **153**, 60
- McLaughlin, D. B. 1924, *ApJ*, **60**, 22
- Mills, S. M., & Mazeh, T. 2017, *ApJ*, **839**, L8
- Mishra, L., Alibert, Y., Udry, S., et al. 2023, *A&A*, **670**, A68
- Muñoz, D. J., & Perets, H. B. 2018, *AJ*, **156**, 253
- Narita, N., Fukui, A., Kusakabe, N., et al. 2019, *J. Astron. Telesc. Instrum. Syst.*, **5**, 015001
- Pepe, F., Cristiani, S., Rebolo, R., et al. 2021, *A&A*, **645**, A96
- Pichierrri, G., Batygin, K., & Morbidelli, A. 2019, *A&A*, **625**, A7
- Queloz, D., Eggenberger, A., Mayor, M., et al. 2000, *A&A*, **359**, L13
- Rein, H., & Liu, S. F. 2012, *A&A*, **537**, A128
- Rice, M., Wang, S., & Laughlin, G. 2022, *ApJ*, **926**, L17
- Rice, M., Wang, X.-Y., Wang, S., et al. 2023, *AJ*, **166**, 266
- Ricker, G. R., Winn, J. N., Vanderspek, R., et al. 2015, *J. Astron. Telesc. Instrum. Syst.*, **1**, 014003
- Rodríguez, J. E., Becker, J. C., Eastman, J. D., et al. 2018, *AJ*, **156**, 245
- Rossiter, R. A. 1924, *ApJ*, **60**, 15
- Sedaghati, E., Jordán, A., Brahm, R., et al. 2023, *AJ*, **166**, 130
- Siegel, J. C., Winn, J. N., & Albrecht, S. H. 2023, *ApJ*, **950**, L2
- Terquem, C., & Papaloizou, J. C. B. 2007, *ApJ*, **654**, 1110
- Teyssandier, J., Libert, A. S., & Agol, E. 2022, *A&A*, **658**, A170
- Turrini, D., Schisano, E., Fonte, S., et al. 2021, *ApJ*, **909**, 40
- Wong, K. H., & Lee, M. H. 2024, *AJ*, **167**, 112
- Zak, J., Bocchieri, A., Sedaghati, E., et al. 2024, *A&A*, **686**, A147
- Zieba, S., Kreidberg, L., Ducrot, E., et al. 2023, *Nature*, **620**, 746

## Appendix A: Simultaneous photometry

Simultaneous photometry was secured on the night of the transit at various facilities: the SARA-CT Andor Ikon-L instrument at the SARA telescope (Keel et al. 2017, 2021) and a 17-inch privately owned telescope on Cerro Pichasca at the Deep Sky Chile observatory; the DFOSC instrument mounted at the ESO 1.54 m Danish telescope (Andersen et al. 1995) and the E152<sup>7</sup> telescope at La Silla; an automated 24-inch telescope at Van Vleck Observatory at Wesleyan University in Connecticut, USA; and the MuSCAT2 (Narita et al. 2019) instrument mounted on the

Telescopio Carlos Sánchez in the Canary Islands. In all cases, the data were reduced with standard procedures, and we used DAOPHOT in its `astropy` implementation to perform differential photometry of HD 110067 and the bright neighboring star TYC 1448-459-1.

From our obtained photometry, we can rule out any significant stellar activity at the level of a few ppt on the night of the transit. However, due to the low expected transit depth of planet c ( $\sim 0.8$  ppt) and the large airmass during the observations, we are unable to detect the planetary transit signal in our simultaneous photometry observations.

---

<sup>7</sup> <https://www.eso.org/public/teles-instr/lasilla/152metre>

Appendix B: Additional figures

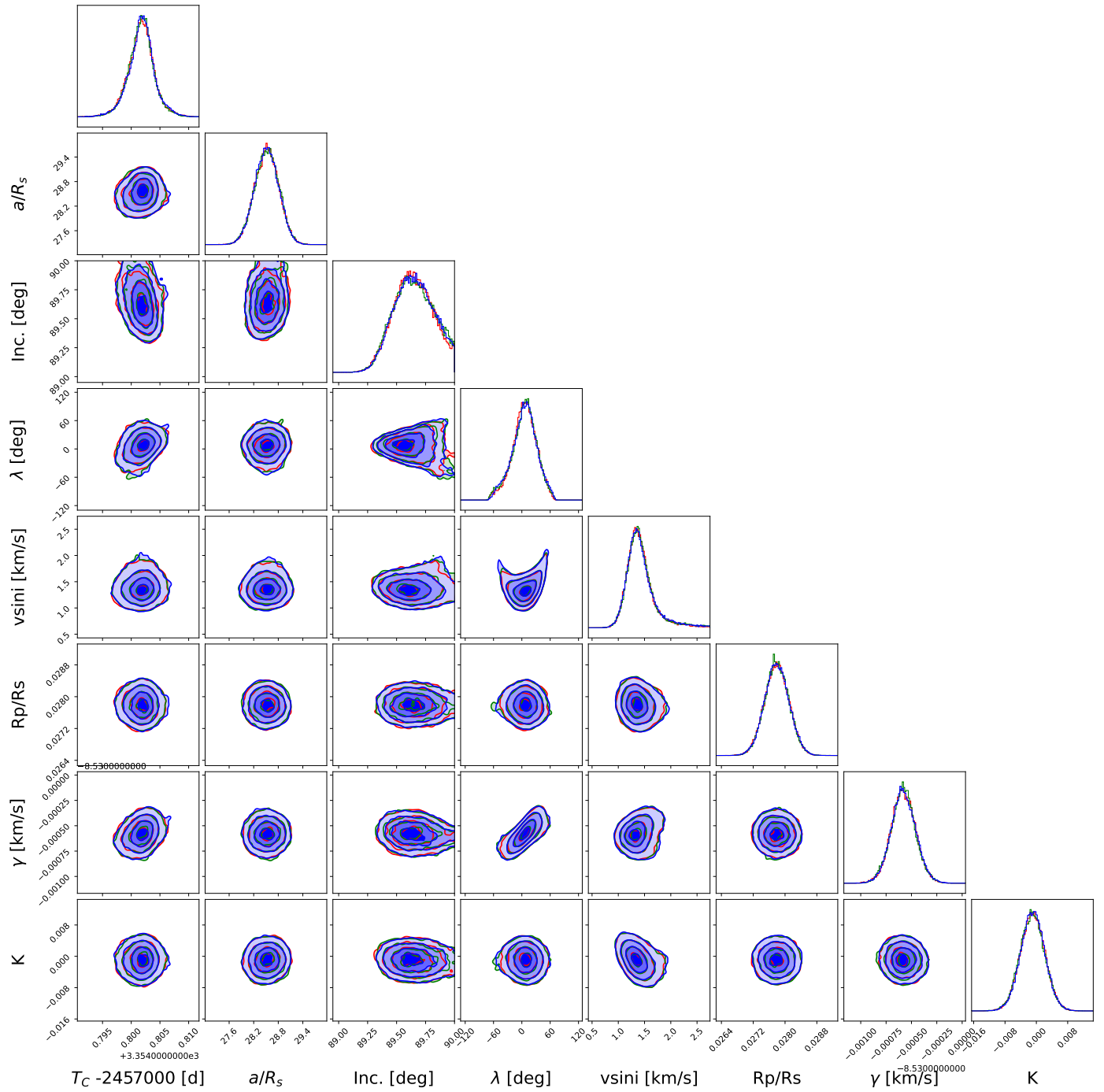
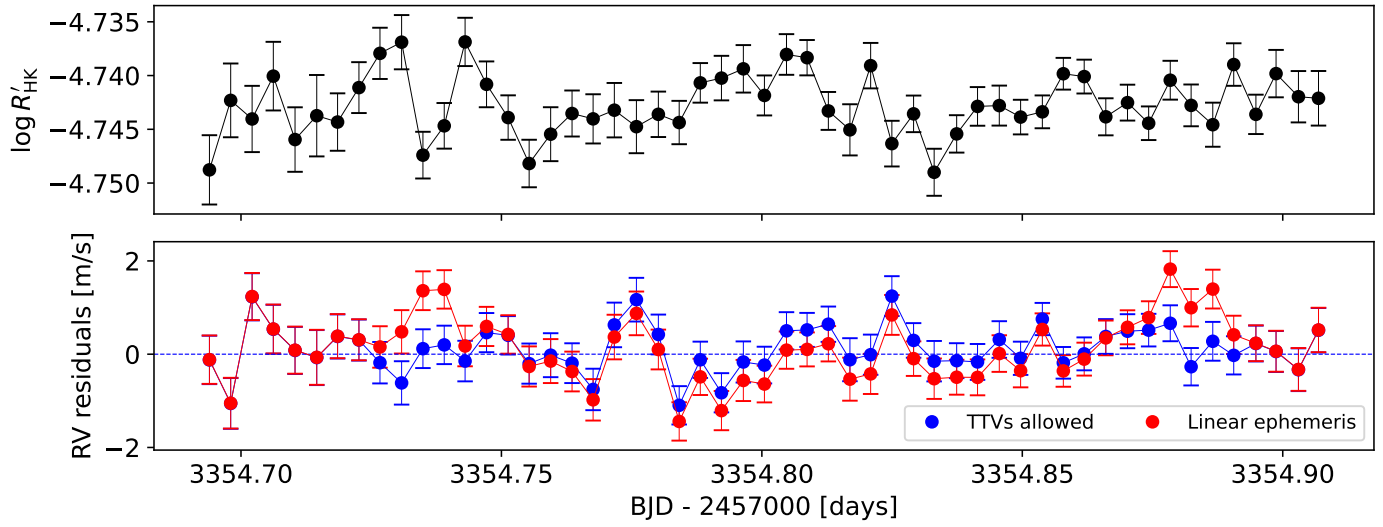


Fig. B.1. Corner plot of the MCMC analysis. Three independent MCMC simulations are shown in different colors.



**Fig. B.2.** Influence of Stellar Activity on Radial Velocity. (*Top*) Values of the  $\log R'_{\text{HK}}$  activity index throughout the night. This index is derived from the calcium H and K lines and is indicative of chromospheric activity. The low scatter indicates that stellar activity does not significantly influence the obtained RV dataset. (*Bottom*) RV residuals after subtracting our R-M effect model from the observed data (blue) and RV residuals after subtracting the R-M effect model with a linear ephemeris (red; Luque et al. 2023). The blue model is preferred due to the lower standard deviation.